International Journal of Medicine Sciences
www.medicinejournal.in
Online ISSN: 2664-889X, Print ISSN: 2664-8881
Received Date: 01-02-2019 Accepted Date: 02-03-2019; Published: 09-03-2019
Volume 1; Issue 2; 2019; Page No. 01-08

Ethanol oxidation of palladium supported on TiO_2Nanoparticle

Mohammed AhmedHusseinAwad[1*], Nabil AN Alkadasi[2]
[1] Chemistry Department, Faculty of Applied Sciences, Thamar University, Thamar, Yemen
[2] Faculty of Engineering, Thamar University, and Faculty of Education and Science Albaida University, Yemen

Abstract
In this paper, TONPs powder (titanium oxide nanoparticles powder) is prepared by anodization in 0.7 M $HClO_4$is annealed in N_2 at 450°C for 3 h to obtain the TONPs-N_2 powder as catalyst support to which Pdis loaded by photodeposition technique using $PdCl_2$ and isopropanol as sacrificial donor. The resulting Pd-TONPs-N_2 powder catalyst exhibits high surface area of 98m^2/g. The catalyst support TONPs arrays powder are electrochemically characterized in basic solution of ethanol by cyclic voltammetry (CV), and chronoamperometry measurements. Pd-TONPs-N_2 powder electrode catalyst exhibits a remarkably high electrocatalytic activity and has high electrocatalytic stability for ethanol electrocatalytic oxidation reaction. Pd supported on the conductive support TONPs-N_2 is used as electro catalyst in fuel cells.

Keywords: Ethanol oxidation, titanium oxide nanoparticles, photo deposition, Pdelectrocatalyst, chronoamperometry

Introduction

Direct ethanol fuel cells (DEFCs) are electrochemical devices that directly convert the chemical energy stored in liquid ethanol into electricity. Based on the electrolyte used, DEFCs can be divided into two types: acid-type DEFCs and alkaline-type DEFCs. Over the past several years, attention has been focused on acid-type DEFCs, and significant progress has been made in their development [1–5]. For example, Mohammed. AH Awad*et al* developed a method for Pd loading on TiO_2 nanoparticles and nanotubes using photodeposition technique for the methanol oxidation reaction (MOR) in a basic medium [1, 2]. Xin *et al*. [3, 4] developed a highly active PtSn catalyst for the ethanol oxidation reaction (EOR) in an acid medium, and they further demonstrated that a maximum power density of over 60mWcm^{-2} could be achieved with this catalyst, which is the highest performance reported in the open literature [3].

Although the performance seems appealing, the commercialization of acid-type DEFCs still remains a problem. One of the most critical issues with this type of fuel cell is that a considerable amount of Pt is needed to achieve decent performance. As Pt is scarce and expensive, the high loading of Pt in electrodes is a critical obstacle limiting the wide commercialization of acid-type DEFCs [3–5].

On the other hand, it has recently been demonstrated that some non-Pt catalysts for the ethanol oxidation reactions and the oxygen reduction reactions (ORR) can be exploited in alkaline media. Alkaline-type DEFCs have consequently attracted increasing attention [6–11].

In alkaline-type DEFCs, Pd-based catalysts can be an alternative to the Pt-based catalyst for the alcohol oxidation reactions in alkaline media [12]. Takamura *et al*. [12–14] found that Pd catalysts exhibited high electrocatalyticactivity to the methanol oxidation reaction (MOR) in the alkaline electrolyte. They further studied the kinetics of the MOR and suggested that the dehydrogenation of the methanol occurred quickly and the rate-determining step (r.d.s.) was the oxidative removal of the methoxiradicals by the hydroxide ions. Shen *et al*. [15–17] prepared a series of Pd-based catalysts and found that Pd catalysts exhibited higher activity and stability than did Ptcatalysts in the EOR in alkaline solutions.

They also demonstrated that the incorporation of an oxide, such as NiO and Ce_2O_3, as the support of the Pd catalyst was favorable to the EOR. The improvement in the activity was attributed to the enhanced anti-poisoning ability of the catalyst resulting from the introduction of the oxide. Literature review reveals that although Pd catalysts can be alternatives to Pt catalysts for the EOR in alkaline media, the catalytic activity, selectivity, and stability of a pure Pd catalyst are critical issues that need to be addressed so that the performance of such catalysts can be improved. To this end, it is essential to gain a better understanding of the reaction mechanism of the EOR on the Pd catalyst. The objective of this work is to study the mechanism of the EOR on Pd using the cyclic voltammetry (CV) method. Based on the CV results and the final product analysis, we propose a reaction sequence and the rate-determining step.

Pd is a suitable low-cost transition metal, about 50 times more abundant in earth than Pt and possesses high catalytic activity towards methanol and ethanol oxidation in alkaline media [18]. Recently, Pd-based catalysts including Pd-oxide composite catalysts [19] and Pd-based binary [20–23] and ternary catalysts [24] have been investigated. For example, Pd-Co (8:1)/C catalyst synthesized by Shen *et al*. [22] exhibited higher electro-catalytic activity and better stability for formic acid oxidation than those of Pd/C catalyst. It was also found that the ball-milled CNTs-

supported Pd–Co (8:1) catalyst was synthesized with better catalytic activity.

Table 1 lists the theoretical energy densities of several fuels compared with those of gasoline and biodiesel. Methanol and ethanol have been under extensive and intensive study as anode fuels, leading to direct methanol fuel cells (DMFCs) and direct ethanol fuel cells (DEFCs), respectively. The electrode reactions are given by [25]:

$$CH_3OH + H_2O \rightarrow CO_2 + 6\,H^+ + 6e^-\ E_0 = 0.016\ V \quad (1)$$

$$C_2H_5OH + 3H_2O \rightarrow 2CO_2 + 12H^+ + 12e^-\ E_0 = 0.085\ V \quad (2)$$

Combined with the standard electrode potential of oxygen reduction reaction (E_0 = 1.229 V), the ideal potential (E^{eq})for DMFC and DEFC are 1.213 V and 1.144 V, respectively.

This study surveys the mechanism of methanol oxidation reaction (MOR), (EOR) and (GOR) using cyclic voltammetry. This is an attempt to deposit the Pd on TONPs-N_2 powder surface and compare results with Pd deposited on TONTs-N_2 powder. It reveals that palladium nanoparticles arrays are promising electro catalysts for MOR in alkaline media.

The forward scan peak current (I_p) and the peak current ratio of the backward to forward scan (I_b/I_f) are critical parameters to estimate the behavior of the catalyst in the alcohols electrooxidation. Largely a higher current density value will provide a greater working current of the fuel cell, whereas a smaller (I_b/I_f) value point to higher catalytic efficiency and well tolerance to the poisoning species arising from the formation of the carbonaceous intermediates on the catalyst through the reaction [26].

Table 1: Energy density of different fuels.

Raw materials	KWh/L	KWh/Kg
Gasoline	9.50	12.89
Biodiesel	9.17	11.72
Ethanol	6.67	8.33
Glycerol	6.26	4.96
Methanol	4.33	5.47
Glucose	6.64	4.32

2. Experimental

2.1 Materials

Table 2: Used materials.

Series	Material
1	Ti foils (>99.5% purity, Alfa Aesar, thickness: 0.25 mm)
2	perchloric acid $HClO_4$
3	Palladium (II) chloride ($PdCl_2$, Sigma– Aldrich, 99.9+ %) as precursor
4	isopropanol (99.0 %) as sacrificial donor($CH_3CHOHCH_3$)
5	potassium hydroxide
6	Ethanol (CH_3CH_2OH)

2.2 Synthesis of Pd-TONPs-N_2 powder

At the beginning titanium oxide nanoparticles powder (TONPs powder) is prepared by the electrochemical anodic oxidation (annodization process). The Ti foils (>99.5% purity, Alfa Aesar, thickness: 0.25 mm) are anodized in an aqueous solution containing0.7 M per chloric acid $HClO_4$ using a two-electrode electrochemical cell (Ti foil as the anode and Pt foil as the cathode) at 20V for 1h at room temperature then, we separate the precipitate (TONPs powder) from the mixed solution using centrifuge. Then dry the precipitate in oven at 80 °C for overnight, then use pestle and mortar to make smooth powder to obtain TONPs powder. The TONPs powders were subsequently annealed at 450 °C in N_2 for 3hs with heating and cooling rates of 5 °C min^{-1} to obtain TONPs-N_2 powder(surface area 109m^2/g). Photo deposition by UV-400W lamp is carried out in an aqueous solution contains 150 mg of TiO_2 NPs powder, 10 ml of 20 mM $PdCl_2$, 10 ml of 0.3 M isopropanoland put in the beaker magnetic stirrer for 2hs. In this step we note change in the colour of the solution in the case of palladium from the yellow colour to the light green colour and this evidence that palladium is deposited on the surface of TONPs-N_2 powder. Then, we separate the precipitate (e.g. Pd adsorbed on TONPs-N_2 powder) from the mixed solution using centrifuge. Then dry the precipitate in oven at 80 °C for overnight, then use pestle and mortar to make smooth powder. Then to prepare the ink; weigh 50 mg of (Pd-TONPs-N_2powder) and add to it 1ml DI water plus 20 μL of nafion (5 wt. %) solution to stick the catalyst on the Au working electrode. After that, we load 3 $\mu l\ of$ the catalyst (Pd-TONPs-N_2powder) by micropipette on 3 mm Au polycrystalline working electrode to carry out cyclic voltammetry (CV).

2.3 Physicochemical characterizations

Transmission electron microscopy (TEM) images are obtained using a JEOL JEM-2100F electron microscope operating at 200 kV.

2.4. Electrochemical measurements

Cyclic Voltammetry (CV)

CV is performed in a conventional three-electrode single-compartment Pyrex glass cell using a computerized potentiostat/galvanostat (Autolab, FRA2, μAUTOLAB, TYPE III). The reference and auxiliary electrodes are SCE and pure Pt-foil, respectively. All potentials provided in the text are based on the SCE electrode only. A Pt wire auxiliary electrode and a saturated calomel reference electrode (SCE) are used. Also 3mm Au polycrystalline working electrode is used (with geometric surface 0.07 cm^2). The software program used in cyclic voltammetry measurements are NOVA 1.9. An evenly distributed suspension ink of catalyst is prepared by ultrasonic the mixture of 50 mg catalyst and 1 mL D.I water for 30 min, and 3 μL of the resultant suspension is laid on the surface of Au polycrystalline working electrode (3 mm diameter, 0.07 cm^2). After drying at 40 °C, 1 μL of Nafion (5 wt. %) solution is covered on the catalyst surface and allowed to dry again. Thus, the working electrode is obtained, and the specific loading of metal on the Au working electrode surface was about 0.0555 mg (55.5μg). Electrochemical tests areperformed in 2 M KOH + different concentrations of ethanol.

Chronoamperometry (CA) is carried out in different potentials i.e. at -0.6V, 0.5V, 0.4V, 0.3V, 0.2V, 0.1V.

3. Results and discussion

3.1 Physicochemical Characterization of Pd-TONPs-N_2 powder catalyst

The TEM images (Fig.1 and Fig. 2) approve the formation of Pd-TONPs-N_2 powder catalyst without varying the original morphology of TONPs. It is also further confirmation for the palladium particles size.

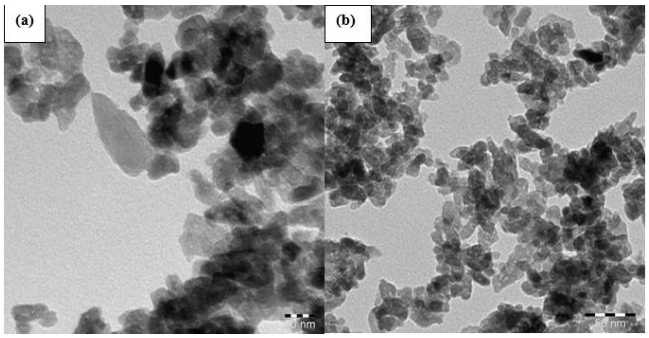

Fig 1: TEM (Transmission electron microscopy) image of TONPs powder annealed in nitrogen (a) 20 nm and (b) 50 nm.

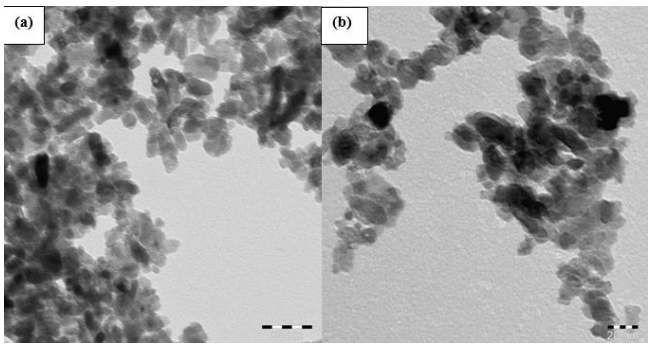

Fig 2: (a) TEM image of Pd-TONPs-N_2 powder; (b) magnified image of Pd-TONPs-N_2 powder.

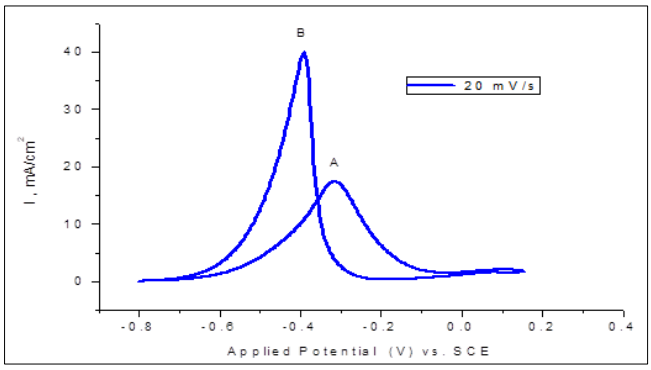

Fig 3: CV for Pd supported on TONPs powder loaded on 3 mm diameter Au polycrystalline working electrode in (2 M KOH+1M ethanol), at scan is 20 mV/s, catalyst loading is 3μl by current density.

Fig.3 shows the cyclic voltammetry of the Pd supported on TiO_2 nanoparticles in 2.0 M KOH solution containing 1.0 M EtOH. The hydrogen desorption/sorption region (<−0.7 V) is significantly suppressed in the presence of ethanol in the solution. The ethanol oxidation reaction starts at −0.8 V and a current peak (designated as Peak A) centered at −0.32V is observed during the forward scan. In the reverse scan, another current Peak B is found centered at about−0.39 V. In the hydrogen region, the suppression of the peak can be attributed to the dissociative adsorption of ethanol in the low-potential region, i.e.:

$Pd + OH^- \leftrightarrow Pd-OH\ ads + e^-$ (3)
$Pd-OH\ ads + OH^- \leftrightarrow Pd-O + H_2O + e^-$ (4)
$Pd-O + H_2O + 2e^- \leftrightarrow Pd + 2OH^-$ (5)
$Pd-OH\ ads + Pd-OH\ ads \leftrightarrow Pd-O + H_2O$ (6)
$Pd + CH_3CH_2OH \leftrightarrow Pd-(CH_3CH_2OH)\ ads$ (7)
$Pd-(CH_3CH_2OH)\ ads + 3OH^- \rightarrow Pd-(CH_3)\ ads + 3H_2O + 3e^-$ (8)

The resultant ethoxi, such as (CH_3CO)ads, is strongly adsorbed onto the active sites of the Pd TiO_2 nanoparticles electrode, which blocks the ab/adsorption of hydrogen, thereby reducing the hydrogen peaks. The steady-state oxidation current of Peak A can only be observed when the potential is above−0.7 V, well above the starting potential of the adsorption of the hydroxyl ions (Eq. (3)). This fact indicates that the adsorbed intermediates, which are formed during the dissociative adsorption of ethanol, can be stripped off the Pd TiO_2 nanoparticles electrode by the adsorbed oxygen-containing species (Pd-OHads). As a result, the EOR can proceed continuously such that the current continues to increase with the potential. At −0.32 V, the current reaches the maximum value and then starts to decline with a further increase in the potential. Previous studies suggested that the decrease in current was related to the formation of the Pd (II) oxide layer on the surface of the electrode at higher potentials (Eqs. (4) and (5)) [27–31].

The formation of the oxide layer can block the adsorption of the reactive species onto the Pd TiO_2 nanoparticle electrode surface and lead to a decrease in the electrocatalytic activity. As the positive-going sweep proceeds, more Pd (II) oxide covers the surface of the electrode. Consequently, the oxidation current of the EOR is further decreased with the increase in the potential. When the potential is above 0.2 V, the oxidation current nearly coincides with the base current in the supporting electrolyte solution, indicating that the EOR that occurs on the fully developed Pd oxide layer is negligible. Fortunately, the decrease in the electrocatalytic activity can be recovered during the negative-going sweep, as evidenced by the presence of Peak B at about −0.41 V. This reactivation can be attributed to the reduction of the Pd (II) oxide (Eq. (6)), which is similar to the behavior observed with the Pt-based catalyst.

Fig. 4 indicates to palladium supported on titanium oxide nanoparticles as a catalyst for ethanol oxidation reaction (EOR). It is observed that the peak current is improved for catalyst synthesized by photodeposition of $PdCl_2$ on TONPs-N_2 powder as support/catalyst using 0.3 M isopropanol. In Fig. 4, concerning the 1 M ethanol concentration at a scan rate is 50mV/s in basic medium, the peak current density in the forward scan for Pd-TONPs-N_2 powder catalyst is measured to be 26.65mA/cm^2 in alkaline medium whereas the peak current density in the backward scan is measured to be 52.9mA/cm^2.

The Pd-TONPs-N_2 powder catalyst which is examined show a considerably enhanced ethanol oxidation activity as compared to TONPs-N_2 powder catalyst support. The ratios of peak currents related to the anodic peaks in forward (I_f) and reverse (I_b) is mostly used to refer to the catalyst tolerance to intermediates created through the ethanol oxidation reaction [32]. A low I_f/I_b

ratio shows poor electro oxidation of ethanolto carbon dioxide during the forward scan, and too much accumulation of carbonaceous intermediates on the catalyst surface [33]. For Pd-TONPs-N_2 powder, the value of I_f/I_b was 0.504 which is smaller than that reported for Pt/carbon (0.75) [32].

Fig.4 displays the effect of the scan rate for ethanol oxidation reaction (EOR) at Pd-TONPs-N_2 powder catalyst in 2 M KOH in the existence of 1 M ethanol. The curve indicates that the anodic current for ethanol oxidation at Pd-TONPs-N_2 powder catalyst increases speedily with increasing the potential scan rate and anodic potential shift toward higher potential values. In reality the time window for ethanol oxidation process at higher scan rates becomes very narrow where facile electron transfer happens among ethanol and catalytic sites. The proportionality of anodic peak currents to the scan rate in a range of 10-150 mV/s was illustrated inFig.5. The anodic peak current are linearly proportional to the scan rate that proposes the total oxidation of ethanol at this electrode is controlled through the ethanol diffusion from solution to surface redox sites [33-35].

Fig.4displays the effect of scan rate for Pd-TONPs-N_2 powder electrode in a potential range from (-0.8 V to 0.15 V) recorded at different scan rate for 1 M ethanol in basic medium (2 M KOH) solution, Fig.4shows an enhanced cathodic and anodic peak current that increase linearly with increasing scan rate, this performance is characteristic of an electrochemical reaction organized by a diffusion process.

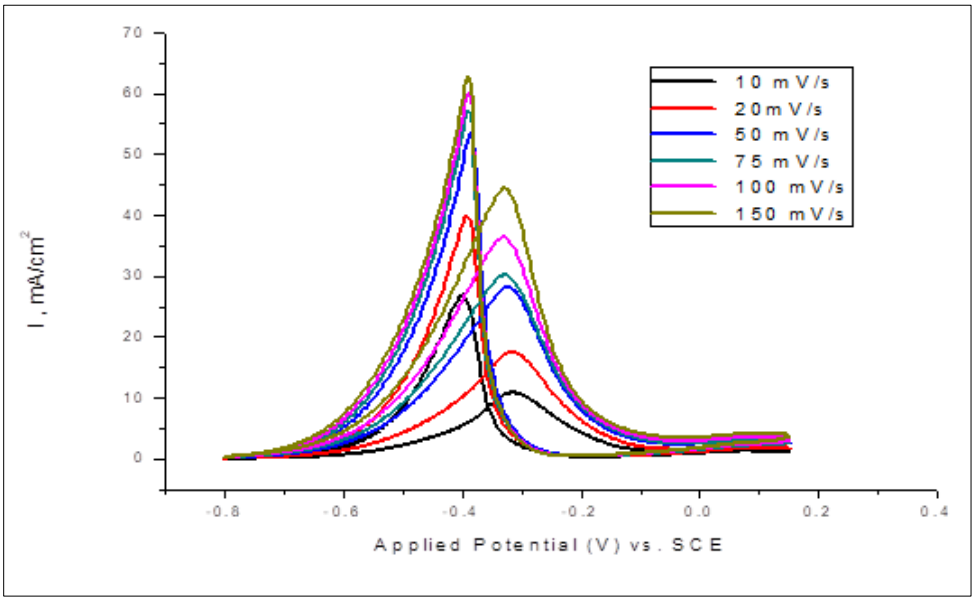

Fig 4: CV for Pd supported on TONPs powder loaded on 3 mm diameter Au polycrystalline working electrode in (2 M KOH+1M ethanol), at different scan rate, catalyst loading was 3μl by current density.

High current density and low I_b/I_f were achieved, which can be ascribed to the large surface area, excellent poisoning tolerance and reduced diffusion resistance. The concentration of both KOH and ethanol affect the forward scan peak current density and the peak position. Particularly, the peak potential depends on the ratio of the KOH concentration to ethanol concentration which affects the ethanol electrooxidation in terms of peak potential and the forward and backward scan peak current densities. Moreover, it is also found that higher E_{upper} could efficiently eliminate the poisoning species through forward scan.

From Fig.5, it is observed that the forward and backward paths are linear and this indicates that the methanol oxidation reaction is controlled by diffusion process.

Table 3: The scan rate (mV/s) and $\sqrt{scanrate}$ ($\sqrt{mV/s}$) vs. I_p (peak height –mA/cm^2) for both the forward and backward paths also contains the values of I_f/I_b for the Pd-TONPs-N_2 powder catalyst loaded on Au working electrode 50 cycles in (2 M KOH + 1M ethanol) (EOR).

Scan (mV/s)	$\sqrt{scanrate}(\sqrt{\frac{mV}{s}})$	I_f (mA/cm^2)	I_b (mA /cm^2)	I_f/I_b
10	3.162	10.510	32.550	0.396
20	4.472	16.430	39.280	0.444
50	7.071	26.650	52.900	0.504
75	8.660	30.180	56.920	0.530
100	10	36.170	59.890	0.604
150	12.247	44.163	66.034	0.669

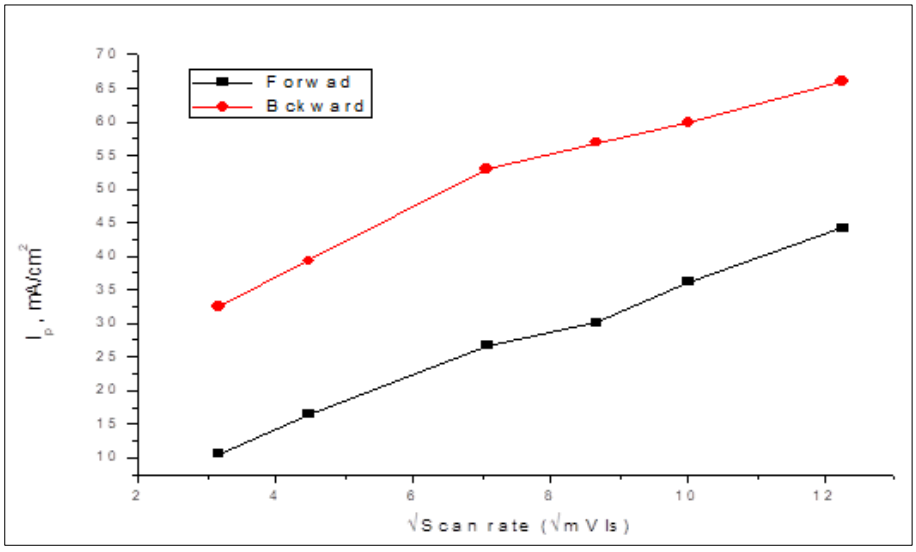

Fig 5: I_p(peak height-mA/cm^2) vs. the $\sqrt{\text{scan rate}}$ ($\sqrt{(mV/s)}$) for both forward and backward paths of Pd-TONPs-N_2 powder in (2M KOH+1 M ethanol)**.**

Fig. 6shows the catalytic stability of the Pd-TONPs-N_2 powder catalyst from 10 cycles to 50 cycles in (2 M KOH + 1 M ethanol) (EOR) with a scan rate of50mV/s. We observe the peaks of the forward increase with increasing the number of crossing steps (number of cycles). Stability test is performed for Pd-TONPs-N_2 powder catalyst. Fig.6 shows the CVs for Pd-TONPs-N_2 powder catalyst after continuous cycling between (-0.8 V and 0.15 V) for a total of 50 cycles. The catalytic stability of Pd-TONPs-N_2 powder catalyst for ethanol oxidation reaction (EOR) is examined by CV as shown in Fig. 6. The Pd-TONPs-N_2 powder ethanol oxidation current shows a steady decrease in current density within the first few cycles (10 cycles) and then an approximately constant current density is progressively recognized for longer time especially in forward. Therefore, the results reveal that Pd-TONPs-N_2 powder possesses high catalytic activity and stability in alkaline media of ethanol.

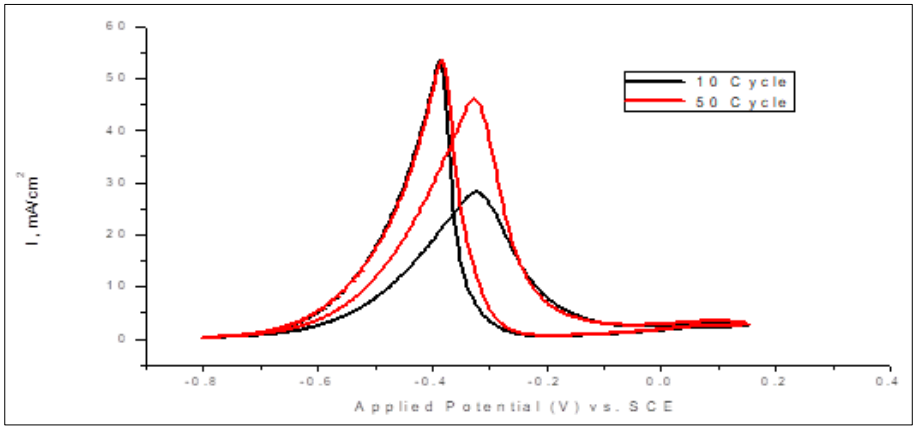

Fig 6: CV Pd-TONPs-N_2 powder catalyst loading 3 µL, 50 cycle and 10 cycle, on Au working electrode, all in (2M KOH+1M ethanol) at a scan rate of 50 mV/s by current density.

Fig. 7 shows the CA of Pd-TONPs-N_2 powder loaded on 3 mm diameter Au working electrode in (2 M KOH+ 1M ethanol) at different potentials (-0.6V,-0.5V,-0.4V, and -3.1 V).

At the principal step of the chronoamperometry curves, the current density is comparatively high owing to the adhesion of ethanol molecules on the active sites. Then the current density decrease when the time increases. Approximately 200 s later, the curve becomes stable. It is well recognized that there are two probable causes for decrease of catalyst activity thru increasing time. First, the rate of intermediate desorption is slower than that of ethanol oxidation, so toxic intermediates would gather on the active sites. Second, catalyst nanoparticles commonly suffer from coarsening which result in disintegration of active sites through the catalytic process.

The stable current density of the Pd-TONPs-N_2 powder at the potential -0.35 V is the highest between the other potentials showing that this would accomplish equilibrium among catalytic activity and poison resistance because of suitable deposition quantity of Pd nanoparticles.

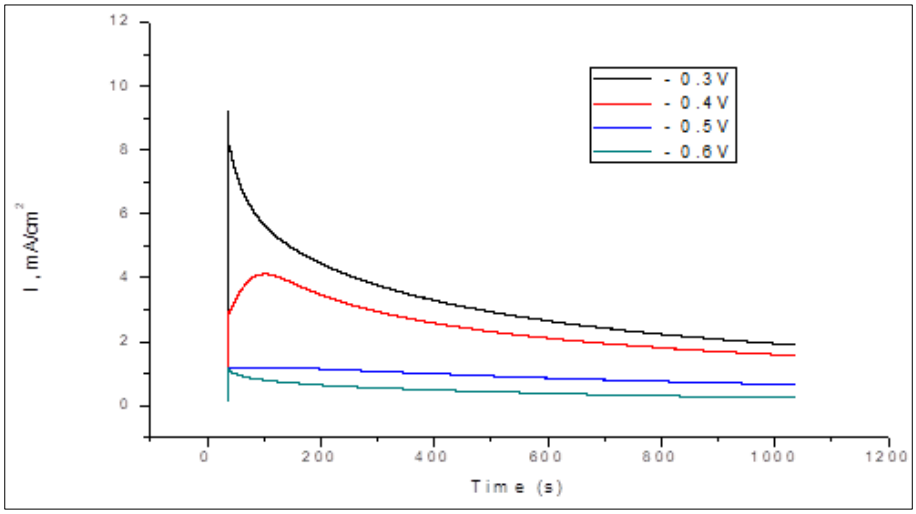

Fig 7: Chronoamperometry for Pd-TONPs-N_2 powder loaded on 3 mm diameter Au working electrode in (2 M KOH+ 1M ethanol).

From Fig.8, it is observed that ethanol electrooxidation for Pd-TONPs-N_2 powder catalyst hashigher for both forward and backward scan current densities than that of methanol electrooxidation for the same catalyst. It means that Pd-TONPs-N_2 powder in ethanol electrooxidation (EOR) has higher catalytic activity than that of the same catalyst in methanol electro oxidation (MOR).

Ethanol possesses has continuously been identified as the most attractive alcoholic fuel for the following reasons. First, ethanol can be conveniently produced from renewable agricultural products, such as corn, sugar, and fruits, by well-established fermentation technology. Second, ethanol is much less toxic and a lot more biodegradable than methanol and fossil fuel. Third, ethanol has a large energy density and a reasonable molecule size compared to any other alcohols. Therefore, it is of great economic and environmental interest to develop an ethanol-fueled, energy-conversion device. From Table 4, it is noted that I_f/I_b ratio for Pd-TONPs-N_2 powder (2.88) in MOR is higher than that of Pd-TONPs-N_2 powder (0.504) in EOR, indicating to different systems.

Also, it is noted that I_b/I_f ratio for Pd-TONPs-N_2 powder (0.35) in MOR is lower than that of Pd-TONPs-N_2 powder (1.99) in EOR and that is due to two different systems.

In the system (2 M KOH +1 M methanol) the forward peak current density of Pd-TONPs-N_2 powder is 21.3mA/cm^2 and the backward peak current density for the same catalyst is 7.4mA/cm^2. On the other hand, in the system (2 M KOH +1 M ethanol) the forward peak current density of Pd-TONPs-N_2 powder catalyst is 26.65mA/cm^2 and the backward peak current density for the same catalyst is 52.9mA/cm^2.

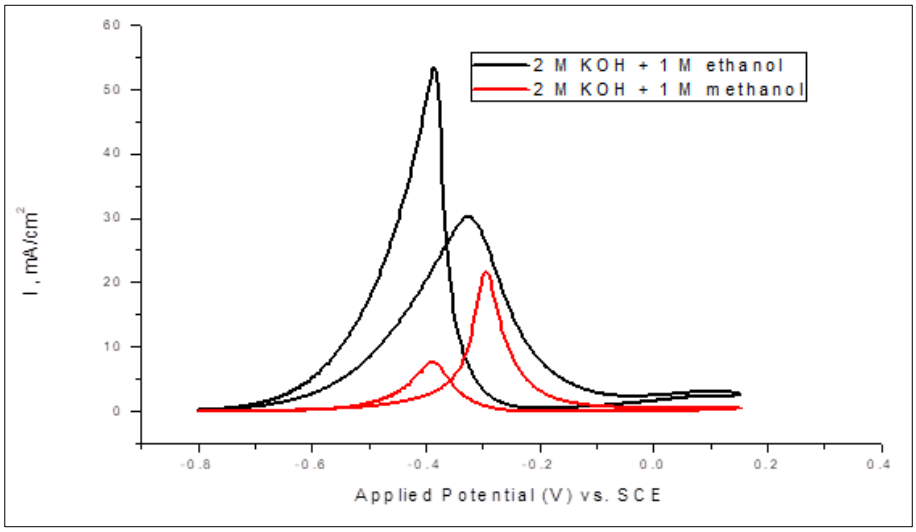

Fig 8: Comparison between CV for Pd-TONPs-N_2 powder loaded on 3mm diameter Au working electrode at a scan rate of 50mV/s by current density in (2 M KOH + 1 M C_2H_5OH) and in (2 M KOH + 1M CH_3OH).

Table 4: The composition ofI_f, I_b, I_b/I_f and $I_f/I_b$of Pd-TONPs-N_2 powder for MOR and EOR.

Catalysts	I_f (mA/cm^2)	I_b(mA/cm^2)	I_f/I_b	I_b/I_f
Pd-TONPs-N_2 powder for MOR	21.30	7.40	2.88	0.35 [1]
Pd-TONPs-N_2 powder for EOR	26.65	52.90	0.504	1.99

In the system (2 M KOH +1 M ethanol) the forward peak current density of Pd-TONPs-N_2 powder is 26.65mA/cm^2 and the backward peak current density for the same catalyst is 52.9mA/cm^2. On the other hand, in the system (2 M KOH +1 M ethanol) the forward peak current density of Pd-PC 500 TiO_2 powder catalyst is 23.52mA/cm^2 and the backward peak current density for the same catalyst is 47.36mA/cm^2.

Table 5: Comparison between the catalysts supports of TONPs-N_2 powder and PC 500 TiO_2 powder. PC500 have a high surface area and high purity ultrafine TiO_2 powder.

Properties	TONPs-N_2 powder	PC 500 TiO_2 powder
Surface area	99 m^2/g	350 m^2/g
Electrocatalytic activity for Pd on catalyst support	High current density	Low current density
Price	Expensive	Cheaper

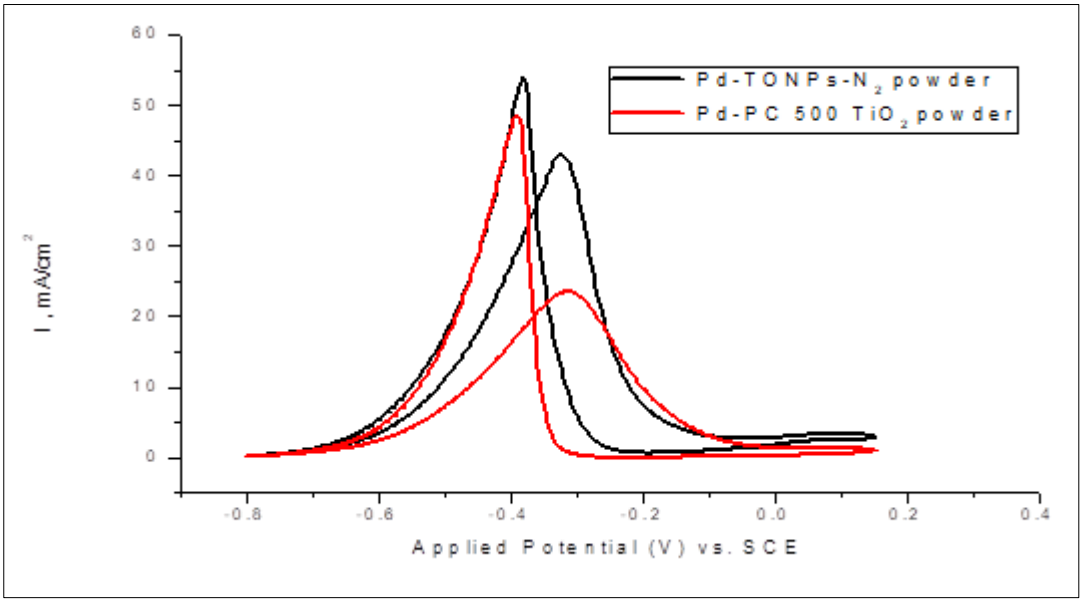

Fig 9: Comparison between CV for Pd-TONPs-N_2 powder and Pd-PC 500 TiO_2 powder, 3 microliter loaded on 3 mm diameter Au polycrystalline working electrode, at a scan rate of 50 mV/s in (2 M KOH+1M ethanol) by current density.

Table 6: The composition of I_f, I_b and I_b/I_f of Pd-TONPs-N_2 powder and Pd-PC 500 TiO_2 powder for EOR.

Catalysts	I_f (mA/cm^2)	I_b(mA/cm^2)	I_f/I_b	I_b/I_f
Pd-PC 500 TiO_2 powder	23.520	47.360	0.497	2.010
Pd-TONPs-N_2 powder for EOR	26.650	52.900	0.504	1.990

4. Conclusions

In summary, Pd NPs are chemically photo deposited on TONPs-N_2 catalyst support, which is prepared by anodization in 0.7 M per chloric acid electrolyte for 60 min then annealed in N_2. In other words, palladium is photo deposited onto TONPs-N_2 powder to produce Pd-TONPs-N_2 powder as electrocatalyst that has high electrocatalytic activity. The Pd-TONPs-N_2 powder electrocatalyst shows a uniform and well dispersion of Pd nanoparticles through TONPs-N_2. This is ascribed to the synergistic effect of TONP catalyst support and palladium nanoparticles and on carbon monoxide (CO) oxidation, the order unidirectional structure of TONPs and the larger conductivity and electrochemical active surface area of the TONPs-N_2. Pd-TONPs-N_2 catalysts are applied in electrocatalysis ethanol oxidation reaction (EOR). This study surveys (EOR) using cyclic voltammetry. The results reveal that palladium nanoparticles arrays are promising electrocatalysts used for (EOR) in basic media.

5. Acknowledgement

The author (Mohammed.A.H.Awad) would like to utilize this opportunity to express his gratitude to Professor Nabil Alkadasi for his non-stop guidance; support throughout the last two years.

6. References

1. Nabil AN, Alkadasi Awad MA, Ghanem MA, Al-Mayouf AM. Palladium supported on titanium oxide nanoparticles as a catalyst for methanol oxidation reaction. International Journal Of Chemistry Studies. 2018; 2(3):10-16.
2. Mohammed AH, Awad Nabil AN. Alkadasi Abdullah M.

Al-Mayouf. Photodeposition of Palladium Supported on TiO2 Nanotubes Powder as Electro catalyst forMethanol Oxidation Reaction.
3. Al-Rayan Journal of Humanities & Applied Sciences. 2018; I:I. Zhou WJ, Song SQ, Li WZ, Zhou ZH, Sun GQ, Xin Q, Douvartzides S, P. Tsiakaras, J. Power Sources. 2005; 140:50.
4. Song SQ, Zhou WJ, Liang ZX, Cai R, Sun GQ, Xin Q, Stergiopoulos V, Tsiakaras P. Appl. Catal. B: Environ. 2005; 55:65.
5. Coutanceau C, Demarconnay L, Lamy C, Leger JM, Power J. Sources. 2006; 156:14.
6. Matsuoka K, Iriyama Y, Abe T, Matsuoka M, Ogumi Z. Power Sources. 2005; 150:27.
7. Shen PK, Xu CW, Zeng R, Liu YL. Electrochem. Solid State Lett. 2006; 9:A39.
8. Bagchi J, Bhattacharya SK. J. Power Sources. 2007; 163:661.
9. Paul P, Bagchi J, Hattacharya SK. Indian J. Chem.: Sect. A. 2006; 45:1144.
10. Rao V, Hariyanto C, Cremers Stimming U. Fuel Cells. 2007; 7:417.
11. Ogumi Z, Matsuoka K, Chiba S, Matsuoka M, Iriyama Y, Abe T, Inaba M. Electrochemistry. 2002; 70:980.
12. Takamura T, Minamiya K, Electrochem J. Soc. 1965; 112:333.
13. Takamura T, Mochimar F. Electrochim. Acta. 1969; 14:111.
14. Takamura T, Sato Y. Electrochim. Acta. 1974; 19:63.
15. Hu FP, Chen CL, Wang ZY, Wei GY, Shen PK. Electrochim. Acta. 2006; 52:1087.
16. Xu CW, Shen PK, Liu YL. J. Power Sources. 2007; 164:527.
17. Shen PK, Xu CW. Electrochem. Commun. 2006; 8:184.
18. Singh RN, Singh A. Anindita, Carbon. 2009;47(1):271.
19. He Q, Chen W, Mukerjee S. S. Chen, Fe. Laufek, J. Power Sources. 2009; 187(2):298.
20. Yu H, Zhou D, Zhu H. J. Solid State Electrochem. 2014; 18(1):125.
21. Almeida TS, Palma LM, Morais C, Kokoh KB, Andrade ARD. J. Electrochem. Soc. 2013'; 160(9):965.
22. Shen SY, Zhao TS, Xu JBE. lectrochim. Acta. 2010; 55(28):9179.
23. Maiyalagan T, Viswanathan B, Varadaraju UV, Nanosci J. Nanotechnol. 2006; 6(7):2067.
24. Su PC, Chen HS, Chen TY, Liu CW, Lee CH, Lee JF, Chan TS, Wang KW0 Int. J. Hydrog. Energy. 2013; 38(11):4474.
25. Vielstich W. A. Gasteiger. Wiley: Oxford, 2009, p 2 v.
26. Zhu LD, Zhao TS, Xu JB, Liang ZX. Journal of Power Sources. 2009; 187(1):80-84; (b) S. Patra, N. Munichandraiah. Langmuir. 25 (3) (2009) 1732-1738.
27. Bagchi J, Bhattacharya SK. Transit. Met. Chem. 2007; 32:47.
28. Prabhuram J, Manoharan R, Vasan HN. J. Appl. Electrochem. 1998; 28:935.
29. Grden M, Kotowski J, Czerwinski A. J. Solid State Electrochem. 2000; 4:273.
30. Grden M, Czerwinski A. J. Solid State Electrochem. 2008; 12:375.
31. Liang ZX, Zhao TS, Xu JB, Zhu LD. Electrochimica Acta. 2009; 54:2203-2208.
32. Wu YN, Liao SJ, Liang ZX, Yang LJ, Wang RF. J. Power Sources. 2009; 194:805-810.
33. Wu JJ, Tang HL, Wan ZH, Ma WT. Electrochim. Acta. 2009; 54:1473-1477.
34. Nukumizu K, Nunoshige J, Takata T, Kondo JN, Hara M. Chem. Lett. 2003; 32:196-197.
35. Allen J. Bard. John Wiley and Sons Inc, New York, L.R.F, 2001.